



Comparison of N₂O₅ mixing ratios during NO₃Comp 2007 in SAPHIR

H. Fuchs^{1,2,*}, W. R. Simpson³, R. L. Apodaca³, T. Brauers⁴, R. C. Cohen⁵, J. N. Crowley⁶, H.-P. Dorn⁴, W. P. Dubé^{1,2}, J. L. Fry^{5,**}, R. Häsel⁴, Y. Kajii^{7,***}, A. Kiendler-Scharr⁴, I. Labazan⁶, J. Matsumoto^{7,****}, T. F. Mentel⁴, Y. Nakashima⁷, F. Rohrer⁴, A. W. Rollins⁵, G. Schuster⁶, R. Tillmann⁴, A. Wahner⁴, P. J. Wooldridge⁵, and S. S. Brown¹

¹National Oceanic and Atmospheric Administration, Earth System Research Laboratory, Boulder, CO, USA

²Cooperative Institute for Research in the Environmental Sciences, University of Colorado, Boulder, CO, USA

³Department of Chemistry and Biochemistry and Geophysical Institute, University of Alaska Fairbanks, Fairbanks, AK, USA

⁴Institute of Energy and Climate Research, IEK-8: Troposphere, Forschungszentrum Jülich GmbH, Jülich, Germany

⁵Department of Chemistry, University of California Berkeley, Berkeley, CA, USA

⁶Max-Planck-Institute for Chemistry, Mainz, Germany

⁷Department of Applied Chemistry, Tokyo Metropolitan University, Tokyo, Japan

* now at: Institute of Energy and Climate Research, IEK-8: Troposphere, Forschungszentrum Jülich GmbH, Jülich, Germany

** now at: Chemistry Department, Reed College, Portland, OR, USA

*** now at: Graduate School of Global Environmental Studies, Kyoto University, Kyoto, Japan

**** now at: Faculty of Human Sciences, Waseda University, Saitama, Japan

Correspondence to: H. Fuchs (h.fuchs@fz-juelich.de)

Received: 19 June 2012 – Published in Atmos. Meas. Tech. Discuss.: 19 July 2012

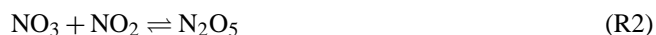
Revised: 5 October 2012 – Accepted: 20 October 2012 – Published: 16 November 2012

Abstract. N₂O₅ detection in the atmosphere has been accomplished using techniques which have been developed during the last decade. Most techniques use a heated inlet to thermally decompose N₂O₅ to NO₃, which can be detected by either cavity based absorption at 662 nm or by laser-induced fluorescence. In summer 2007, a large set of instruments, which were capable of measuring NO₃ mixing ratios, were simultaneously deployed in the atmosphere simulation chamber SAPHIR in Jülich, Germany. Some of these instruments measured N₂O₅ mixing ratios either simultaneously or alternatively. Experiments focused on the investigation of potential interferences from, e.g., water vapour or aerosol and on the investigation of the oxidation of biogenic volatile organic compounds by NO₃. The comparison of N₂O₅ mixing ratios shows an excellent agreement between measurements of instruments applying different techniques (3 cavity ring-down (CRDS) instruments, 2 laser-induced fluorescence (LIF) instruments). Datasets are highly correlated as indicated by the square of the linear correlation coefficients, R^2 , which values were larger than 0.96 for the entire datasets.

N₂O₅ mixing ratios well agree within the combined accuracy of measurements. Slopes of the linear regression range between 0.87 and 1.26 and intercepts are negligible. The most critical aspect of N₂O₅ measurements by cavity ring-down instruments is the determination of the inlet and filter transmission efficiency. Measurements here show that the N₂O₅ inlet transmission efficiency can decrease in the presence of high aerosol loads, and that frequent filter/inlet changing is necessary to quantitatively sample N₂O₅ in some environments. The analysis of data also demonstrates that a general correction for degrading filter transmission is not applicable for all conditions encountered during this campaign. Besides the effect of a gradual degradation of the inlet transmission efficiency aerosol exposure, no other interference for N₂O₅ measurements is found.

1 Introduction

The nitrate radical, NO₃, and its reservoir species dinitrogen pentoxide, N₂O₅, play an important role in nocturnal chemical processes (Wayne et al., 1991). NO₃ is a major oxidant for pollutants during the night and contributes to the oxidative capacity of the atmosphere. Reactions of NO₃ and N₂O₅ drive numerous chemical cycles in the nocturnal atmosphere, including the removal of nitrogen oxides (e.g. Brown et al., 2004), production of organic and inorganic nitrate (e.g. Atkinson and Arey, 2003), and halogen activation (Osthoff et al., 2008; Thornton et al., 2010; Phillips et al., 2012). These nocturnal processes impact the ozone formation potential on the following day (e.g. Brown et al., 2006) and the formation of secondary aerosol (Fry et al., 2009; Riemer et al., 2003). NO₃ is the product of the reaction of ozone, O₃, with nitrogen dioxide, NO₂. N₂O₅ is formed by the further reaction of NO₃ with NO₂, but is thermally labile, so that NO₃ and N₂O₅ concentrations are often in a thermal equilibrium (equilibrium constant K_{eq}):



$$[\text{N}_2\text{O}_5] = K_{\text{eq}}[\text{NO}_3][\text{NO}_2] \quad (1)$$

NO₃ and N₂O₅ are abundant only at night, because NO₃ is easily photolyzed and undergoes rapid reaction with NO present during daytime. Nighttime N₂O₅ mixing ratios are highly variable with maximum mixing ratios of a few parts per billion by volume (ppbv) (e.g. Brown et al., 2007).

NO₃ has been detected by optical absorption spectroscopy for several decades using (1) differential optical absorption technique (DOAS) (Platt et al., 1980) and (2) matrix-isolation ESR spectroscopy (MI-ESR) (Mihelcic et al., 1993; Geyer et al., 1999). During the last decade, new techniques for atmospheric NO₃ detection have been applied: cavity-based absorption spectroscopy (see reviews Brown, 2003; Ball and Jones, 2003) and laser-induced fluorescence (LIF) (Wood et al., 2003; Matsumoto et al., 2005). Stratospheric NO₃ has also been detected by remote measurements techniques (e.g., from the ground Allan et al., 2002, or from satellite Kyröllä et al., 2010).

Because N₂O₅ can be thermally decomposed to NO₃, closed cavity-based techniques and LIF also allow quantification the sum of NO₃ and N₂O₅ by using a heated inlet and heated detection cell. Direct detection of N₂O₅ can also be accomplished by chemical ionization spectroscopy (CIMS) (Slusher et al., 2004; Kercher et al., 2009).

Quality assurance of measurements is an important task, especially for recently developed techniques like those for NO₃ and N₂O₅. One way to accomplish such quality assurance, is to compare concurrent measurements by different instruments. In summer 2007, a large set of instruments detecting NO₃ and/or N₂O₅ measured synthetic gas mixtures

designed to produce NO₃ and N₂O₅ and potential interfering species during eleven days of experiments in the atmosphere simulation chamber SAPHIR in Jülich, Germany. This was the first attempt to compare instruments applying cavity-based absorption techniques (5 instruments for NO₃, 3 instruments for N₂O₅ + NO₃), LIF (2 instruments for NO₃ + N₂O₅), and DOAS (1 instrument for NO₃). No CIMS instrument took part in this campaign. The results of the comparison of NO₃ measurements are discussed by Dorn et al. (2012). In addition, comparison of NO₂ concentrations, measured by a number of instruments, have already been presented (Fuchs et al., 2010a). Detection of the sum of peroxy nitrates ($\sum\text{PNs}$), total alkyl and multifunctional nitrates ($\sum\text{ANs}$) and nitric acid by a thermal dissociation LIF instrument (Day et al., 2002) were used for the interpretation of the fate of reactive nitrogen species during experiments that investigated the degradation of VOCs by NO₃ and associated secondary aerosol formation (Rollins et al., 2009; Fry et al., 2009, 2011). In this paper, the comparison of N₂O₅ measurements is discussed.

2 Experimental setup

2.1 Cavity ring-down spectroscopy

Several instruments using cavity-based absorption techniques participated in this campaign. All instruments measured NO₃ absorption at its absorption maximum at 662 nm. In addition, three cavity ring-down instruments had the capability to detect N₂O₅ by its conversion to NO₃. The instruments from the National Oceanic and Atmospheric Administration, US, (NOAA-CRDS) and the University of Alaska Fairbanks, US, (UAF-CRDS) contain two separate cavities allowing to detect NO₃ and the sum of N₂O₅ and NO₃ simultaneously. The instrument from the Max-Planck-Institute for Chemistry in Mainz, Germany, (MPI-CRDS) had only one measurement channel during this campaign, which could be switched between NO₃ and N₂O₅ + NO₃ detection. Because there was no fast switching between these two modes, the instrument ran in either one of the modes during any given experiment. The operators chose to measure N₂O₅ + NO₃ only during two of the eleven experiments.

The principles of cavity ring-down spectroscopy for NO₃ are discussed elsewhere (Brown, 2003). Details of the NOAA-CRDS instrument can be found in Dubé et al. (2006); Osthoff et al. (2006); Fuchs et al. (2008). The version of the instrument that operated during the comparison campaign in 2007 was based on pulsed laser CRDS. This instrument has since been converted to a diode laser based instrument (Wagner et al., 2011). Aspects of the instrument that affect its accuracy, such as the inlet system and calibration methods, are similar to those described here. The UAF-CRDS instrument is described by Ayers et al. (2005); Ayers and Simpson (2006); Apodaca (2008) and the MPI-CRDS by Schuster

et al. (2009). A summary of the properties of these instruments as operated during this campaign is given in Table 1. Only a short description of instruments will be given here.

Laser light is coupled into a cavity, which consists of two high reflective mirrors in a distance of 70–95 cm. Either a pulsed laser (NOAA-CRDS) or a laser diode (UAF-CRDS, MPI-CRDS), which is periodically turned on and off, provides light at 662 nm. The spectral modes of the laser and the cavity modes must match to couple the light into the cavity efficiently. In the NOAA-CRDS, a short laser pulse provides a dense spectrum of modes to be coupled into the cavity and is aligned into the cavity on-axis. UAF-CRDS and MPI-CRDS couple the laser light off-axis into the cavity, in order to increase the density of the cavity mode spectrum (Paul et al., 2001).

After the laser pulse has been applied or the laser diode has been switched off, the light that leaks out of the rear mirror of the cavity is observed by a photo multiplier tube (PMT). The time constant of the decaying light intensity gives a direct measurement of the extinction in the cavity, including Rayleigh and Mie scattering, absorption and loss due to the mirror transmission and scattering (Berden et al., 2000). Extinction due to scattering of particles does not play a role in the instruments here, because a Teflon filter (pore size 1–2 μm, sufficient to remove all optically active particles from the sample air flow) is placed in the inlet and prevents particles from entering the cavity. The instruments are zeroed by periodic additions of NO to the inlet. When NO is added, NO₃ is quantitatively converted to NO₂ in its reaction with NO before entering the cavity, so that the NO₃ absorption can be selectively switched on and off:



The NO₃ absorption cross section determined by Yokelson et al. (1994) and the temperature dependence of the cross section by Orphal et al. (2003) was used by all instruments to calculate NO₃ mixing ratios from the measured absorption. Because of the specific titration of NO₃, absorption of other trace gases at 662 nm is included in the zero measurements. ClNO₂ or other halogens compounds likely to be activated from N₂O₅ heterogeneous uptake do not absorb visible light, they are very unlikely to present an interference to any of the optical methods for NO₃ or N₂O₅ detection compared here. More details of the instruments regarding their capability to detect NO₃ and the set-up in the SAPHIR chamber are described in Dorn et al. (2012). One of the major advantages of concentration measurements by absorption is that calibration of the instrument sensitivity is not required.

N₂O₅ is thermally decomposed to NO₃ in the inlet of the instruments downstream of the Teflon filter. The tubing in the inlet and the cavity are heated to 70 to 95 °C, respectively, forcing the equilibrium between NO₃ and N₂O₅ to the NO₃ side. The time needed for quantitative conversion is mainly limited by the time needed to heat the sampled air. Therefore, the conversion time depends on the specific design of

the heater. The NOAA-CRDS and UAF-CRDS heaters consist of two stages, where ambient air flows first through a Teflon converter maintained at 140 °C and 100 °C and then into the measurement cell maintained at 75 °C and 85 °C, respectively. The inlet and cavity of the MPI-CRDS instrument is heated to a constant temperature of 95 °C. If NO₂ concentrations are exceptionally large, the equilibrium between NO₃ and N₂O₅ may not be completely shifted to NO₃. N₂O₅ measurements by NOAA-CRDS were corrected for this effect by calculating (Eq. 1) the maximum N₂O₅ mixing ratio that is not converted to NO₃ at operational conditions. This correction was less than 3 % for most of the experiments, but was 8 % in the morning on 20 June, when the NO₂ mixing ratio reached 80 ppbv.

The major uncertainty of NO₃ and N₂O₅ measurements by CRDS instruments, which use closed cavities, is their inlet transmission efficiencies. The loss of N₂O₅ on Teflon surfaces, of which all instruments are made, is small compared to that of NO₃ (Simpson, 2003; Aldener et al., 2006; Fuchs et al., 2008). However, in order to be detected, N₂O₅ must be thermally decomposed to NO₃, so that NO₃ loss in the cavity needs to be taken into account. In order to minimise the residence time (few hundred milliseconds) of the sampled air in the cavity and thereby the NO₃ loss, the flow rate in the instruments is between 4 and 8 l per minute. The pressure is reduced to approximately 350 hPa in the NOAA-CRDS instrument to further shorten the residence time. In addition to the loss of NO₃, the N₂O₅ mixing ratio can be reduced by heterogeneous uptake, if the inlet system is exposed to particles (Fuchs et al., 2008). In the NOAA-CRDS, the filter was automatically changed. The interval varied between 2 h and 45 min depending on the aerosol concentration expected during a particular experiment. The filter could be manually changed in the UAF-CRDS and MPI-CRDS instruments, so that filter changes were done at most every few hours, but more often once per day during this campaign.

Different methods can be applied to quantify the N₂O₅ loss in the instrument, in order to correct measured N₂O₅ mixing ratios. Here, the N₂O₅ loss in MPI-CRDS and UAF-CRDS was measured by varying the flow rate during occasions when NO₃ and N₂O₅ mixing ratios were approximately constant in the chamber. For MPI-CRDS a sticking coefficient was derived from the reduction of the signal for increasing residence time of the sampled air. The value for the MPI-CRDS instrument was derived from measurement of the NO₃ loss after N₂O₅ decomposition in the hot inlet and cavity (Schuster et al., 2009). A total loss of 10 ± 10 % and 9 % for the measurement of the sum of NO₃ and N₂O₅ was determined for the MPI-CRDS and UAF-CRDS instruments, respectively, for their operational conditions.

The loss of NO₃ and N₂O₅ in the NOAA-CRDS was determined using a different approach. This instrument contains one more cavity, in which NO₂ is detected by CRDS at 532 nm (Dubé et al., 2006; Osthoff et al., 2006). This measurement channel is placed downstream of the cavities for

Table 1. Performance and properties of instruments detecting N₂O₅ during NO₃Comp.

	MPI-CRDS	UAF-CRDS	NOAA-CRDS	UCB-LIF	TMU-LIF
method	off-axis CRDS	off-axis CRDS	pulsed CRDS	fluorescence	fluorescence
laser repetition rate/Hz	200	560	50	c.w.	10000
time resolution/s	5	1 to 2	1	300	720
1 σ precision ^c /pptv	1 ^a	1.4 ^b	1.6 ^b	37 ^b	63 ^d
1 σ accuracy/%	± 13	$\pm 25^e$	± 7	± 20	± 16
filter ^f	Teflon 1–2 μm	Teflon 2 μm	Teflon 2 μm	no filter	no filter
N ₂ O ₅ transmission (tubing)	0.90	0.91	0.98	n.a.	n.a.
N ₂ O ₅ transmission (filter)	1.00	1–0.013/h	1.00	n.a.	n.a.
flow rate/slm	8	8	4	6	2.4
cavity length/m	0.7	0.685	0.93	n.a.	n.a.
mirror reflectivity/%	99.998	99.995	99.9995	n.a.	n.a.
max. ring-down time/ μs	95	95	450	n.a.	n.a.
pressure	ambient	ambient	350 hPa	2.7 hPa	8 hPa
NO ₃ titration frequency	1 min	3 min	3 min	5 min	n.a.

^a Schuster et al. (2009); ^b this work; ^c at the original time resolution; ^d determined from counting statistics of measurements during this campaign;

^e without systematic errors from filter aging and ^f PTFE Teflo, Pall.

NO₃ and N₂O₅. A constant N₂O₅ mixing ratio in zero air from a solid N₂O₅ sample, which is kept at dry ice temperature, is fed into the system. The sampled N₂O₅ mixing ratio is quantified by measuring the NO₂ mixing ratio, if excess NO is added, so that NO₃ produced after thermal decomposition of N₂O₅ in the instrument is converted to NO₂. Because NO₂ loss in the system is negligible, the relationship between changes in the NO₂ and N₂O₅ signals with and without the addition of NO gives the N₂O₅ transmission efficiency of the instrument (Fuchs et al., 2008). An N₂O₅ loss of $2 \pm 3\%$ was measured on four days during this campaign.

Because the N₂O₅ loss is not determined regularly during an experiment, potential changes over the course of an experiment are not monitored. The accumulation of particles in the system, especially on the filter in the inlet, can lead to a variable, significantly higher N₂O₅ loss than determined in the characterisations experiments described above. For example, Fuchs et al. (2008) estimated an increase of N₂O₅ loss of 2% per hour, if the filter is exposed to ammonium sulfate aerosol at humid conditions for the NOAA-CRDS instrument. The filter in the NOAA-CRDS instrument was automatically changed regularly for this reason. All measurements by UAF-CRDS were corrected for an increasing N₂O₅ loss with the filter age by an empirical function, which assumes that N₂O₅ loss increased linearly by 1.3% per hour. This correction and a 9% N₂O₅ loss at zero filter age was derived by fitting the filter transmission as a function of age in hours for nine filters used during this comparison campaign. The N₂O₅ loss in the instrument was measured by the flow variation method. The 9% N₂O₅ loss at zero filter age represents a combination of tubing transmissions and possible loss on an unloaded filter, which was probably dominated by losses other than the filter because the inlet transmission recovered after the filter change. The increase in loss with filter loading is attributed to loading of aerosol onto the filter.

2.2 Laser induced fluorescence

Two instruments making use of LIF participated in this campaign. One from the University of California at Berkeley, California, US, (UCB-LIF) and one from the Tokyo Metropolitan University, Japan (TMU-LIF). Because of technical problems, the TMU-LIF instrument measured only during the last two experiments and the data quality was poorer than normal for this instrument. The UCB-LIF is described in detail by Wood et al. (2003, 2005) and the TMU-LIF instrument by Matsumoto et al. (2005).

The UCB-LIF instrument samples six litres per minute through a critical orifice into two detection cells held near 2.7 hPa. In each detection cell, NO₃ is excited by a multi-mode diode laser near its absorption maximum at 662 nm. The NO₃ fluorescence is detected using a PMT with a red-sensitive GaAs photocathode after passing two 700 nm long-pass interference filters. The laser output is modulated for 45 ns long laser pulses with a duty cycle of 50%. Signal from the long-lasting fluorescence is only acquired shortly after the laser is turned off in order to reduce the amplitude and variability in background from short-duration Raman, aerosol and chamber scatter. Similar to the CRDS instruments, the background is measured regularly by chemically destroying NO₃ in the inlet. In contrast to the NO used for this purpose with the CRDS instruments, isoprene was used to avoid generating excess NO₂ which would produce a small fluorescence signal in this instrument. N₂O₅ is detected as in the CRDS instruments by thermal decomposition to NO₃ in the heated inlet of one of the detection cells, so that the sum of NO₃ and N₂O₅ is measured. To determine the inlet temperature for N₂O₅ detection, thermal scans of the signal from N₂O₅ were performed under high NO₂ conditions resulting in a higher temperature setpoint (170 °C) than is used by the CRDS instruments.

The concept of the TMU-LIF instrument is the same as for the UCB-LIF. The major difference is the laser system that provides the light to excite NO₃. A pulsed Nd:YVO₄ laser pumps a dye laser to produce laser light at the 623 nm NO₃ absorption band. Unfortunately, the laser system did not operate for most of the time during this campaign. Only during the last two experiments was the output powerful enough to detect NO₃ albeit with less sensitivity compared to the performance achieved in previous reports (Matsumoto et al., 2005). NO₃ fluorescence is detected by gated, single photon counting with a time-delay after the laser excitation. The wavelength of the laser is periodically switched between on- and off-resonance wavelengths in order to account for background signals, such as laser stray light and fluorescence from NO₂, which is also excited at 623 nm. Like the other instruments, the inlet of the TMU-LIF is equipped with a heater, which is operated at 85 °C, in order to convert N₂O₅ to NO₃.

In contrast to CRDS instruments, the sensitivity of the LIF instruments needs to be calibrated. The UCB-LIF calibration constant was determined in Jülich by quantifying N₂O₅ simultaneously with this instrument, and a separate instrument (NO₂ TD-LIF, Wooldridge et al., 2010) that detects the NO₂ fragment resulting from N₂O₅ thermal decomposition and is calibrated with an NO₂ standard. The NO₃ UCB-LIF instrument was calibrated on one day during the campaign. The pressure dependence of the Stokes Raman scatter was measured hourly during normal instrument operation and used as a proxy for cell alignment to normalise the instrument sensitivity (Wood et al., 2005). Calibration of the TMU-LIF is achieved by sampling from an N₂O₅ source. Like for the UCB-LIF instrument, the N₂O₅ mixing ratio is quantified by measuring the NO₂, but TMU-LIF makes use of its capability to detect NO₂ at the same wavelength as NO₃. The accuracy of this calibration procedure is 20 and 16 % for UCB-LIF and TMU-LIF, respectively.

2.3 Experiments

Experiments were conducted in the atmosphere simulation chamber SAPHIR in Jülich, Germany. A description of the chamber and its properties can be found elsewhere (Rohrer et al., 2005; Bohn et al., 2005). The chamber offers the possibility to investigate chemical processes under atmospheric conditions. Previous instrument comparison campaigns have shown that different instruments sample the same trace gas and radical concentrations from different locations within the chamber providing evidence that SAPHIR is suitable for this type of experiments (Schlosser et al., 2007, 2009; Apel et al., 2008; Fuchs et al., 2009, 2010a,b).

SAPHIR consists of a double wall Teflon (FEP) film of cylindrical shape (length 18 m, diameter 5 m, volume 270 m³). Slight overpressure prevents leakages of outside air into the chamber. The chamber can be exposed to sunlight by opening its roof. For the purpose of this campaign, the shutter

system was only open for short events (duration within the range of minutes), because NO₃, having been the main target species of the campaign, is easily photolyzed by visible light. The chamber is flushed between experiments with ultra-pure zero air, which is mixed from evaporated liquid nitrogen and oxygen (Linde, purity 99.99990 %), so that experiments always start with clean, dry air. Air which is consumed by instruments and small leaks is continuously replenished with zero air leading to a dilution of trace gases at a rate of approximately 5 % per hour. The chamber air can be humidified by evaporating Milli-Q water, which is flushed into the chamber together with a high flow of zero air. It is also possible to flush the chamber with filtered ambient air. This was done for one experiment (11 June). Besides instruments detecting NO₃ and N₂O₅, a number of other instruments measured O₃ (chemiluminescence detector, modified Eco Physics CLD 770AL, Ridley et al., 1992), NO (chemiluminescence detector, Eco Physics CLD 770AL), NO₂ (chemiluminescence detector, LIF, CRDS, Fuchs et al., 2010a), VOC (PTRMS, Ionicon, GC, Perkin Elmer) concentrations, and aerosol properties such as number (CPC, TSI 3785) and surface concentrations, size distribution (SMPS, TSI 3936L85) and their composition (HR-TOF-AMS, Aerodyne Research).

NO₃ and N₂O₅ were produced in the slow oxidation of NO₂ with O₃, which were injected into the chamber from a gas bottle (Linde) and a silent discharge ozonizer, respectively. No NO_x is observed in the clean chamber and after ozone addition to the clean chamber air. No other trace gas was added during three experiments (9, 12, 13 June). On 12 and 13 June, the chamber roof was opened for short periods, in order to observe the photolysis of NO₃. Other experiments were used to test instruments for potential artifacts from water vapour (10 June) and aerosol exposure (15 June) or focussed on the investigation of VOC degradation by NO₃ (isoprene: 18 June, butanal: 14 June, limonene: 16 June, β-pinene: 20 and 21 June). Each experiment was finished by opening the roof, so that NO₃ and N₂O₅ were quickly destroyed. A summary of the experimental conditions is given in Table 2. More details of the experiments are described by Dorn et al. (2012). Details and results of the VOC degradation experiments are also discussed by Rollins et al. (2009) and Fry et al. (2009, 2011).

3 Results

3.1 Time series of N₂O₅ mixing ratios

Figure 1 shows the time series (time is given as UTC throughout this paper) of N₂O₅ measurements for all experiments together with key parameters like NO₂ and O₃. Measurements are averaged to 1 min time intervals for the analysis shown here. All instruments measured the sum of NO₃ and N₂O₅, but UCB-LIF, UAF-CRDS and NOAA-CRDS had a second measurement channel to measure NO₃ mixing

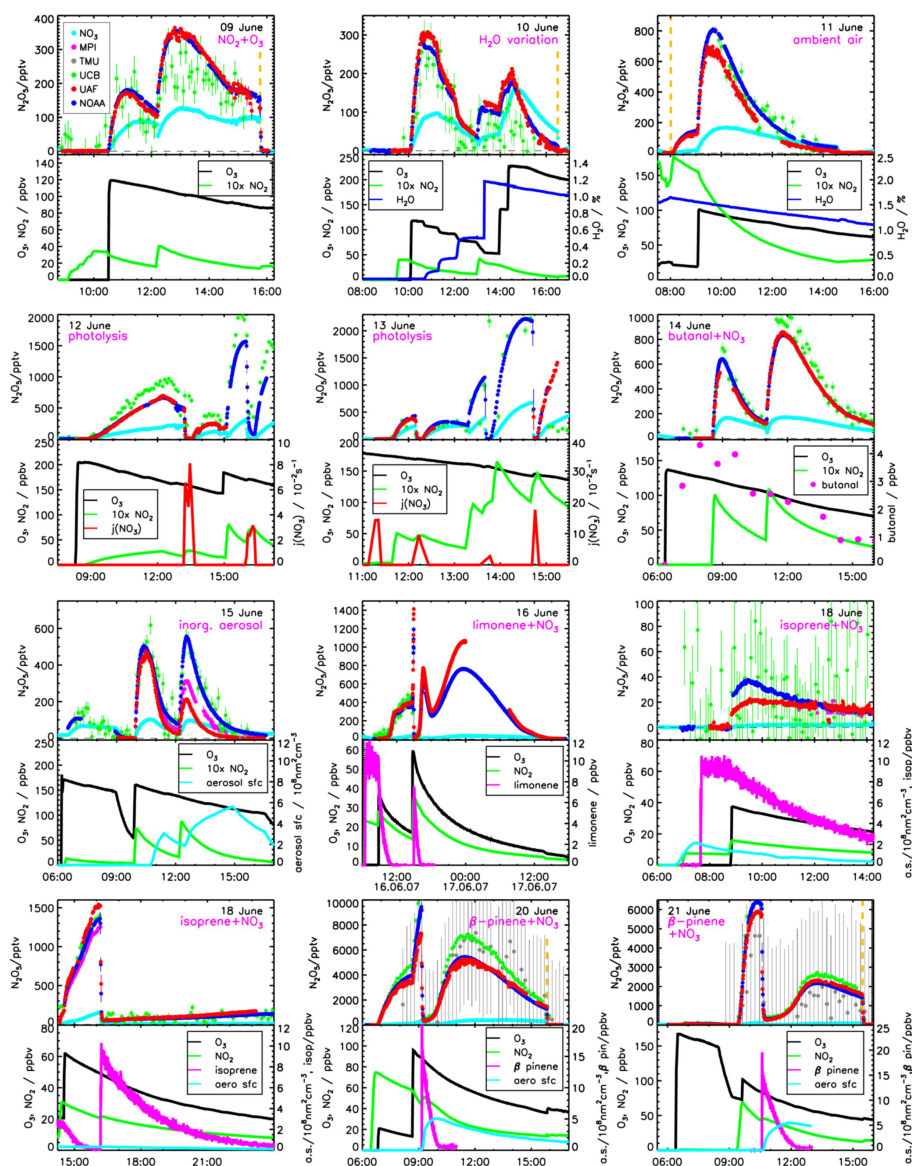


Fig. 1. Diurnal variation of N_2O_5 mixing ratios (1 min average) and compounds which were of importance during the experiment (aero sfc: aerosol surface concentration). NO_3 mixing ratios by NOAA-CRDS were taken to calculate N_2O_5 mixing ratios from the sum measurement by MPI-CRDS, UCB-LIF, and TMU-LIF. The experiment on 18 June is divided into two panels, because N_2O_5 mixing ratios were much higher during the second part of the experiment. Yellow dashed vertical lines indicate opening or closing of the chamber roof, if $j(NO_3)$ is not displayed.

ratios simultaneously. UAF-CRDS and NOAA-CRDS instruments used their own NO_3 measurements to calculate N_2O_5 mixing ratios. The NOAA-CRDS NO_3 measurement, rather than the UCB-LIF NO_3 measurement was used to subtractively determine N_2O_5 for UCB-LIF, because the NOAA-CRDS instrument had significantly higher signal-to-noise in the NO_3 channel. In order to compare N_2O_5 from MPI-CRDS and TMU-LIF, also NO_3 mixing ratios measured by NOAA-CRDS are subtracted from the reported $NO_3 + N_2O_5$ mixing ratios. NOAA-CRDS measurements are chosen, because this instrument had the highest precision and it had

the best data coverage over the campaign. However, results shown here do not depend on the choice of a particular NO_3 measurement, because differences among the instruments measuring NO_3 were rather small (Dorn et al., 2012). Moreover, N_2O_5 mixing ratios were typically two to ten times larger than NO_3 (Fig. 1), so that a potential systematic error from the NO_3 measurement is a somewhat smaller contribution to systematic error in N_2O_5 . Data are excluded for the correlation and regression analysis during rapid changes of the NO_3 mixing ratio (for example during roof-opening events), because the subtraction of slightly

Table 2. Chemical conditions during experiments conducted during the NO₃Comp campaign. Mixing ratios are maximum values during the experiments.

Date	NO ₂ /ppbv	O ₃ /ppbv	NO ₃ /pptv	N ₂ O ₅ /pptv	H ₂ O ^a /%	T ^b /°C	Experiment/test
9 June	4	120	130	350	c	31–32	
10 June	4	230	170	300	0.5	32–36	stepwise change of humidity
11 June	17	100	150	750	1.8	31–37	addition of ambient air
12 June	8	200	400	1600	c	30–31	short photolysis events
13 June	18	200	700	2200	c	29–31	short photolysis events
14 June	12	135	180	850	c	34–37	oxidation of butanal (max. 4 ppbv)
15 June	10	180	120	550	1.8	33–35	addition of inorganic aerosol ((NH ₄) ₂ SO ₄)
16 June	38	60	55	1300	c	29–36	oxidation of limonene (max. 10 ppbv) +CO (max. 500 ppmv)
18 June	33	60	150	1400	1.2	29–36	oxidation of isoprene (max. 10 ppbv) +aerosol ((NH ₄) ₂ SO ₄)+CO (max. 500 ppmv)
20 June	75	100	400	10000	c	33–37	oxidation of β-pinene (max. 20 ppbv)
21 June	70	165	110	6000	1.2	30–33	oxidation of β-pinene (max. 20 ppbv)

^a mixing ratio; ^b inside the chamber and ^c no addition of water vapour.

asynchronous data from the two different instruments could introduce larger systematic errors in these periods. In the MPI-CRDS instrument, the inlet transmission efficiency for NO₃ of approximately 85 % was taken into account in the calculation of N₂O₅ mixing ratios.

The typical N₂O₅ time series (Fig. 1) was characterised by increasing N₂O₅ mixing ratios after NO₂ and O₃ were injected into the chamber resulting from the slow oxidation of NO₂ by O₃. Without further trace gas additions or photolysis events, maximum N₂O₅ mixing ratios were reached after one to two hours. In most of the experiments NO₂ and/or O₃ were added a second time, so that the production of NO₃ and N₂O₅ was further enhanced and a second N₂O₅ maximum was reached (e.g., on 9 June). The N₂O₅ mixing ratio decreased at longer times for several reasons. All trace gases were diluted by approximately 5 % per hour, because of the replenishment of chamber air (see Section Experiments). Moreover, wall loss reactions limited the lifetimes of NO₃ and N₂O₅ to approximately 0.5 and 4 h, respectively, when no NO₃ reactant or aerosol was present (Fry et al., 2009). During other experiments, NO₃ was removed in the chamber by the reaction with VOCs (16, 18, 20 and 21 June) or by photolysis. This led also to a fast decrease of the N₂O₅ mixing ratio due to the establishment of the equilibrium. In addition, N₂O₅ can be directly lost by heterogeneous hydrolysis.

The N₂O₅ time series measured by the different instruments exhibit an overall good agreement with the exception of the second part of the experiment on 15 June, when ammonium sulfate aerosol was present in the chamber. Results of this experiment will be discussed in detail in the next section. Larger differences are also observed on 16 June. Deviations between NOAA-CRDS and UAF-CRDS increase over the course of the experiment (maximum 30 %) before UAF-CRDS measurement stop at midnight. No other N₂O₅ measurement is available for this period. The experiment was

continued over night and on the following day. N₂O₅ mixing ratios by both instruments agree again, when UAF-CRDS measurements restart in the morning after a new filter had been put in the inlet. Another more general feature, which is observed in the time series, is that N₂O₅ mixing ratios measured by UCB-LIF are often larger than those measured by the CRDS instruments as can be seen, for example, on 12 and 20 June, when N₂O₅ mixing ratios by UCB-LIF are approximately 30 % larger than those by the two CRDS instruments.

3.2 Precision of measurements

Measurements before trace gases were added in the morning, when no N₂O₅ is expected to be present in the chamber, give the possibility to analyse the precision of measurements. Figure 2 shows the distribution of “zero” measurements for UAF-CRDS, NOAA-CRDS, and UCB-LIF. The number of measurements for MPI-CRDS and TMU-LIF, which measured N₂O₅ mixing ratios only during two experiments, was too small for this analysis. A Gaussian function is fitted to the distribution, in order to determine its width and centre. The centre gives the bias in the zero measurements, which is much smaller than the width of the distribution for all instruments, demonstrating that there is no significant systematic deviation in the measurements from zero. The width of the distribution is a measurement of the instrument precision (at their time resolution): UAF-CRDS 1.4 pptv (1 to 2 s), NOAA-CRDS 1.6 pptv (1.0 s), UCB-LIF 37 pptv (300 s). These values can be compared to the a priori precisions, which are given by the reported measurement errors. The mean of error bars is plotted in Fig. 2 at the position of the width of the distribution. For UCB-LIF and NOAA-CRDS, the mean of measurement errors agrees with the width of the distribution, whereas it is approximately 50 % larger than the mean of errors for UAF-CRDS. This indicates

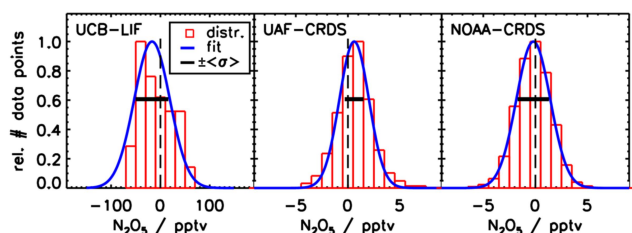


Fig. 2. Distribution of N₂O₅ measurements during times, when instruments sampled zero air from the clean chamber, before trace gases were injected. Only UCB-LIF, UAF-CRDS and NOAA-CRDS provided a sufficiently large number of data points for this analysis. Data are fitted to a gaussian distribution, whose width ($\pm 1\sigma$) is compared to the mean of the measurement errors ($\pm(\sigma)$).

that the precision is well-represented by the reported errors for UCB-LIF and NOAA-CRDS, but is underestimated for UAF-CRDS measurements.

3.3 Regression analysis

The agreement between measurements (1 min average) are analysed more quantitatively by a correlation and regression analysis, for which NOAA-CRDS measurements are taken as reference. However, the results shown here are independent of the choice of the reference. The linear regression takes measurement errors of both coordinates into account (FITEXY procedure in Press et al., 1992, pp. 274–276). The correlation between measurements is generally very high as indicated by the squared linear correlation coefficients. For the entire dataset, R^2 is 0.98, 0.99, and 0.99 for UAF-CRDS, UCB-LIF, and MPI-CRDS, respectively (Table 3). Squared linear correlation coefficients for single experiments are within this range with two exceptions. (1) On the first two experiment days N₂O₅ mixing ratios were close to the precision of the UCB-LIF instrument (maximum N₂O₅ mixing ratio of 350 pptv), so that a worse correlation is expected. (2) As observed in the time series, measurements disagree on 15 June (R^2 is 0.72 and 0.87 for UAF-CRDS and MPI-CRDS, respectively). The low performance of the TMU-LIF instrument resulted in a smaller linear correlation ($R^2 = 0.74$) between NOAA-CRDS and TMU-LIF data compared to the correlation between the other instruments.

Maximum N₂O₅ mixing ratios were variable between different experiments ranging from 300 pptv to 10 ppbv. N₂O₅ mixing ratios were less than 2 ppbv for the majority of experiments (except on 20 and 21 June), similar to the range of N₂O₅ reported from field intensives in the ambient atmosphere. Therefore, Fig. 3 shows the correlation between measurements for all data below 2 ppbv and the entire dataset. Results of the regression analysis are given in Table 3.

The slope of the regression between UCB-LIF and NOAA-CRDS is 1.26 for the entire dataset and 1.18 for the data subset below 2 ppbv. The deviation from unity is

within the combined 1σ accuracies of both instruments and the intercept is below the 1σ precision of the UCB-LIF instrument (Table 1). The slope for individual experiments ranges from 0.97 to 1.35, with the exception of the experiment on 9 June, when the N₂O₅ mixing ratio was close to the limit of detection of the UCB-LIF instrument. The sum of squared residuals is within the range of the number of data points ($\chi^2/(N-2)$ in Table 3) indicating that the relationship of data is consistent with a linear behaviour within the errors. Differences, which are observed between UCB-LIF and NOAA-CRDS (e.g., 20 June), are often similar to the differences between UCB-LIF and UAF-CRDS (Fig. 1). This suggests day-to-day variability of the sensitivity of the LIF instrument.

The slope of the regression between UAF-CRDS and NOAA-CRDS is 1.18 and 1.24 for the entire dataset and all N₂O₅ data below 2 ppbv, respectively. Because of the high precision of measurements by both instruments, a clear change in the agreement between both instruments can be seen over the course of an experiment on 15, 16 and 18 June (Fig. 3), when also the slope of the regression yields largest differences from unity. These deviations from a single linear relationship between data is also reflected by the large values of squared residuals divided by the degree of freedom. Because the reported error bars are within the precision of data (Fig. 2), this behaviour is most likely caused by accuracy problems over the course of an experiment as discussed below. Furthermore, the relationship between UAF-CRDS and NOAA-CRDS becomes nonlinear with increasing N₂O₅ mixing ratios larger than 2 ppbv (Fig. 3), when NOAA-CRDS values are significantly larger than those by UAF-CRDS. However, these data points were collected during only two periods on the last two days.

Measurements between MPI-CRDS and NOAA-CRDS deviate on 15 June (slope of the regression 0.8, Table 3) as expected from the worse correlation, but agree on 18 June (slope of the regression 0.9) within the accuracy of measurements. The agreement between TMU-LIF and NOAA-CRDS is reasonable (slope of the regression 1.1, Table 3) considering the noisy data of the TMU-LIF instrument (Figs. 1 and 3). The poor performance of the LIF laser is reflected by the large error bars of the TMU-LIF measurements and does not allow any further conclusions about the TMU-LIF instrument from this campaign.

4 Discussion

4.1 Correction for filter aging of measurements by UAF-CRDS

The agreement between UAF-CRDS and NOAA-CRDS changed over the course of the experiment on 16 June which was continued over night and the next day (see above). This behaviour can be explained by the correction of data, which

Table 3. Results of the linear regression analysis between N₂O₅ data taking NOAA-CRDS as reference (*a*: slope, *b*: intercept, *R*²: squared correlation coefficient, $\frac{\chi^2}{N-2}$: sum of squared residuals divided by the degrees of freedom, *N*: number of data points). Data are averaged to 1 min time intervals.

Date	UAF-CRDS					UCB-LIF				
	<i>a</i>	<i>b</i> /pptv	<i>R</i> ²	$\frac{\chi^2}{N-2}$	<i>N</i>	<i>a</i>	<i>b</i> /pptv	<i>R</i> ²	$\frac{\chi^2}{N-2}$	<i>N</i>
9 June*	1.008±0.001	−0.3±0.3	0.99	18	239	0.67±0.06	23±12	0.63	2	45
10 June*	1.137±0.001	−4.8±0.2	0.99	15	297	1.16±0.07	−73±10	0.74	2	51
11 June	0.830±0.001	−5.4±0.6	0.99	29	273	0.97±0.03	−26±9	0.91	4	40
12 June*	1.019±0.001	−3.6±0.3	0.99	10	281	1.35±0.01	9±7	0.98	3	65
13 June*	0.906±0.003	1.1±0.9	0.99	5	81	1.18±0.01	−70±16	0.98	6	23
14 June*	1.001±0.002	−7.1±0.7	0.99	8	360	1.15±0.02	−19±8	0.97	2	81
15 June	0.568±0.006	−16.3±0.3	0.72	280	351	1.05±0.03	−13±7	0.90	2	69
16 June	1.308±0.001	−9.6±0.6	0.99	86	1126	1.01±0.04	14±8	0.89	2	49
18 June	1.213±0.002	−5.6±0.3	0.99	38	715	1.05±0.01	−8±4	0.98	2	146
20 June	0.976±0.001	−3±8	0.97	130	456	1.301±0.004	−117±15	0.99	15	80
21 June	1.049±0.001	−9±2	0.99	42	476	1.224±0.005	−26±8	0.99	3	82
comb. all	1.180±0.001	−5.5±1.2	0.98	258	4646	1.260±0.002	−44±2	0.99	6	731
comb. (< 2 ppbv)	1.239±0.001	−11±1	0.95	198	4163	1.178±0.006	−27±2	0.94	4	622
comb.*	1.015±0.001	−1.0±0.6	0.99	20	1258	1.258±0.007	−45±3	0.96	6	265

Date	MPI-CRDS					TMU-LIF				
	<i>a</i>	<i>b</i> /pptv	<i>R</i> ²	$\frac{\chi^2}{N-2}$	<i>N</i>	<i>a</i>	<i>b</i> /pptv	<i>R</i> ²	$\frac{\chi^2}{N-2}$	<i>N</i>
15 June	0.803±0.002	−19.0±0.6	0.87	110	180					
18 June	0.900±0.001	0.1±0.8	1.00	2	123					
20 June						1.2±0.4	−95±1500	0.75	0.1	46
21 June						0.7±0.4	−200±1000	0.85	4200	39
comb. all	0.880±0.001	−10.8±0.4	0.99	112	303	1.1±0.3	−300±900	0.74	0.1	85

* No aerosol addition or significant formation.

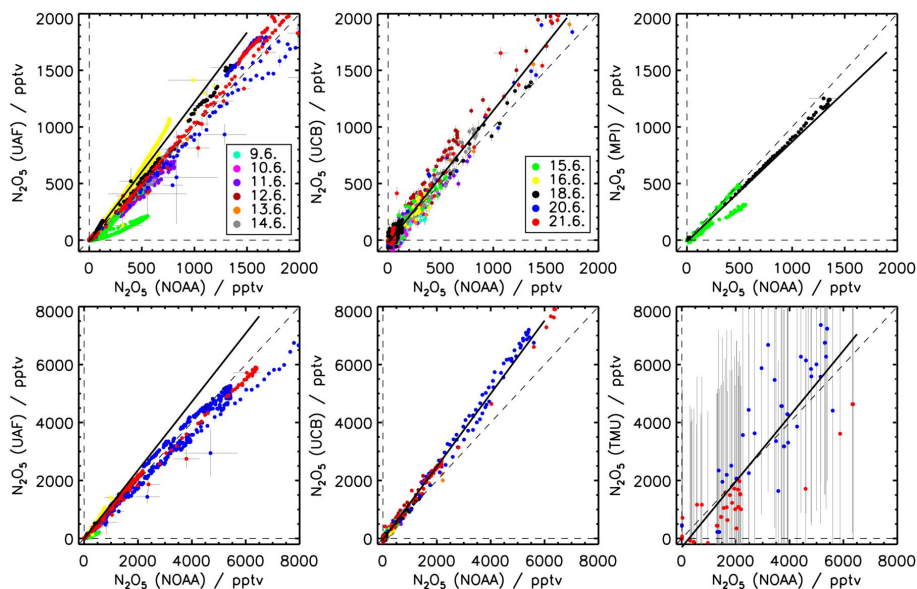


Fig. 3. Correlation between N₂O₅ data from UAF-CRDS, MPI-LIF and TMU-LIF taking N₂O₅ by NOAA-CRDS as reference. The range of N₂O₅ mixing ratios is limited to 2000.pptv in the upper panels, because N₂O₅ mixing ratios were below this value during most of the experiments. Solid black lines give the results of the regression analysis.

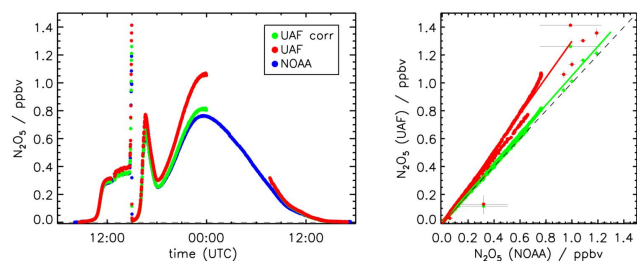


Fig. 4. Time series and correlation of N_2O_5 measurements by UAF-CRDS and NOAA-CRDS on 16 and 17 June (limonene+ NO_3). UAF-CRDS data are either plotted as reported or without a correction factor, which was originally applied to account for an increasing N_2O_5 loss on the filter over time (Table 1). The filter in the UAF-CRDS was exchanged in morning of both days before measurements started. Solid lines in the correlation plot show results from the regression analysis.

was applied to the UAF-CRDS measurement to account for a decrease of the N_2O_5 inlet transmission efficiency (Table 1). The long duration of the experiment allowed to test the validity of the correction, because small errors in the correction accumulated over time (23 % over 18 h measured by UAF-CRDS on 16 June). Figure 4 shows the time series and correlation between UAF-CRDS and NOAA-CRDS for this experiment with and without the correction of the UAF-CRDS data. The large difference between measurements by both instruments in the evening becomes much smaller, if the correction is not applied. This is even more obvious in the correlation plot, which clearly shows that uncorrected data are grouped around one line. In contrast, data which include the correction factor are split into several sub-datasets, which exhibit different, partly nonlinear relationships. The correction is based on several tests of the inlet transmission efficiency (see instrument description above) over 25 h, which show a decrease of 1.3 % per hour. It was assumed that this observation is a general behaviour of the filter in the inlet, which was exchanged once a day before an experiment started. The UAF-CRDS choice of a single time-varying filter degradation model was made because this is the standard operational method for a field campaign for this instrument and, thus, it was applied consistently across the full dataset before data were compared. In a typical field campaign, it is uncommon to have high NO_x pollution without particles on some days and with large particulate loading on others, which was the design of the comparison experiments. Therefore, the over-correction of UAF-CRDS inlet transmission data on some days and undercorrection on others is probably amplified by the experimental design. This amplification clearly exposes the problem of using filters for long periods of time and use of a single linear filter degradation model under conditions where the ratio of aerosol loading to NO_x pollution is highly variable.

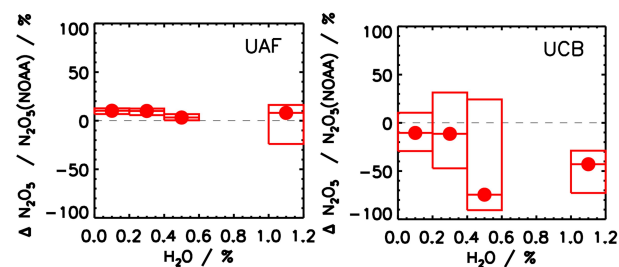


Fig. 5. Statistical analysis of the relative difference of N_2O_5 measurements between UAF-CRDS, UCB-LIF instruments and NOAA-CRDS ($\Delta\text{N}_2\text{O}_5 = \text{N}_2\text{O}_5 - \text{N}_2\text{O}_5(\text{NOAA})$) depending on the water vapour mixing ratio on 10 June (maximum relative humidity 40 %). The water vapour mixing ratio was increased in several steps, which correspond to the boxes shown here. Dots are medians and boxes give the 25 to 75 percentiles of the distribution.

As seen in the time series and correlation plot UAF-CRDS measurements are smaller for very large N_2O_5 mixing ratios up to 8 ppbv on 20 and 21 July. The exact reason of the decreased agreement is not clear.

4.2 Influence of water vapour

The experiment on 10 June was dedicated to investigate potential interferences from water vapour in the N_2O_5 measurements. The water mixing ratio was increased in four steps up to nearly 1.2 %. Artifacts due to water vapour could be caused by its absorption at 662 nm, where the CRDS instruments probe the NO_3 absorption. Figure 5 shows a statistical analysis of the relative difference between UAF-CRDS and UCB-LIF and NOAA-CRDS (MPI-CRDS did not measure N_2O_5 during this experiment). Values below 0.5 pptv are excluded. Dots are median values and boxes give the 25 and 75 percentiles of the distribution. No systematic change in the relationship between measurements with increasing water vapour (up to a mixing ratio of 1.2 % and relative humidity of 40 %) in the chamber is observed, indicating that instruments did not suffer from an interference by water vapour.

4.3 Influence of inorganic aerosol

Measurements between instruments strongly deviate during the experiment on 15 June, when inorganic aerosol (ammonium sulfate) was injected into the chamber starting at 10:45 UTC. A similar statistical analysis as for water vapour is shown in Fig. 6 for aerosol surface concentration during this experiment. Whereas a strong increase in the difference between NOAA-CRDS and MPI-CRDS and UAF-CRDS, respectively, is observed with increasing aerosol surface concentration, the relationship between NOAA-CRDS and UCB-LIF is independent of the aerosol surface concentration. This is also seen in the time series in Fig. 1.

The filter in the inlet system of the NOAA-CRDS was automatically exchanged every 45 min on this day. There are no

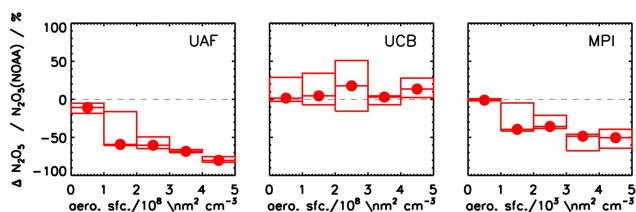


Fig. 6. Statistical analysis of the relative difference of N_2O_5 measurements between UAF-CRDS, MPI-CRDS, UCB-LIF instruments and NOAA-CRDS depending on the aerosol surface concentration during the experiment on 15 June, when ammonium sulfate aerosol was injected into the chamber. Dots are medians and boxes give the 25 to 75 percentiles of the distribution.

discontinuities in the N_2O_5 mixing ratios before and after the filter change. Therefore, it is unlikely that N_2O_5 loss on the filter after 45 min of aerosol exposure affected the measurements. Also the agreement with measurements by the UCB-LIF instrument, which did not have a filter in the inlet system, supports that there are no significant unaccounted N_2O_5 losses in the NOAA-CRDS measurements.

Assuming that NOAA-CRDS and UCB-LIF measurements do not suffer from other artifacts in the N_2O_5 measurements, the strong increase of the relative difference between NOAA-CRDS and UAF-CRDS and MPI-CRDS is most likely caused by a degradation of their inlet transmission efficiencies with increasing aerosol exposure. This could be related to the more infrequent filter changes. In the UAF-CRDS instrument, one filter, which was inserted in the morning, remained in the instrument over the course of the experiment. The filter in the MPI-CRDS instrument was exchanged in the morning and around 13:15 UTC for a second time. Although the difference of MPI-CRDS measurements to NOAA-CRDS and UCB-LIF is slightly smaller after the filter change, a large difference persists. The filter in the MPI-CRDS instruments was placed upstream of the heated part of the inlet, in which N_2O_5 is thermally decomposed, but there was still a 50 cm PFA tubing between the filter and the sampling point in the chamber. Because the filter change does not lead to the full recovery of the inlet transmission efficiency, this inlet tubing is most likely responsible for a major part of the N_2O_5 loss. The inlet line of the NOAA-CRDS upstream of its filter was also nearly 40 cm long, so that a similar effect could be expected. However, the residence time of the sampled air in the NOAA-CRDS instrument is significantly shorter than that in the MPI-CRDS instrument.

If NO_3 and N_2O_5 are in a thermal equilibrium, N_2O_5 mixing ratios can be calculated by Eq. (1). These can be compared to the LIF and CRDS measurements for an independent consistency check. Calculated N_2O_5 mixing ratios are shown in Fig. 7 using NO_2 measurements from a chemiluminescence detector, the measured temperature inside the chamber and NO_3 measurements by either UAF-CRDS or NOAA-CRDS. During the first two hours after the injection

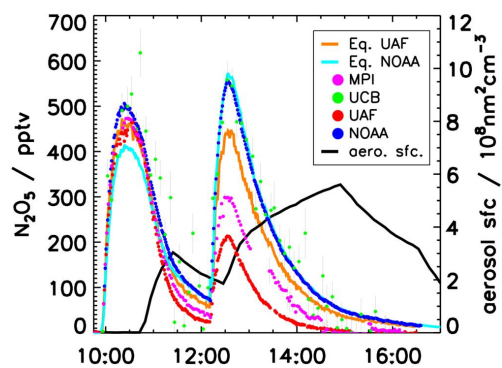


Fig. 7. Comparison of measured N_2O_5 mixing ratios to calculations assuming thermal equilibrium between NO_3 and N_2O_5 on 15 June when ammonium sulfate aerosol was injected into the chamber. N_2O_5 was either calculated from NO_3 measurements from the UAF-CRDS or NOAA-CRDS instrument.

of NO_2 and O_3 (no aerosol present), the calculated N_2O_5 using NOAA-CRDS NO_3 slowly approaches N_2O_5 measurements. In the presence of large amounts of aerosol, calculated N_2O_5 mixing ratios using NOAA-CRDS NO_3 are consistent with measurements by NOAA-CRDS and UCB-LIF. NO_3 mixing ratios measured by NOAA-CRDS were 15 to 20 % smaller compared to measurements by the other instruments during the first part of the experiment (Dorn et al., 2012), but agree at later times, so that the lower N_2O_5 calculated from thermal equilibrium using NO_3 by NOAA-CRDS is most likely due to an under-prediction of NO_3 by NOAA-CRDS. In contrast, calculated N_2O_5 using UAF-CRDS NO_3 is within the range measured values during the first part of the experiment, but measured N_2O_5 by UAF-CRDS and MPI-CRDS is much lower than calculated N_2O_5 by NOAA-CRDS or UAF-CRDS, when ammonium sulfate was present. This comparison to equilibrium indicates that there are N_2O_5 losses in the inlet system of UAF-CRDS and MPI-CRDS instruments during this period. N_2O_5 mixing ratios which are calculated using UAF-CRDS NO_3 are approximately 20 % smaller than those using NOAA-CRDS NO_3 . They are inconsistent with any of the N_2O_5 measurements.

Deviations between the NOAA and UAF instruments on another day with inorganic aerosol addition (18 June) also showed evidence for N_2O_5 loss in the instrument without a frequent filter change. Again, N_2O_5 mixing ratios by UAF-CRDS were smaller than those by NOAA-CRDS after exposure to aerosol, but measurements by both instruments agreed later, when the aerosol surface concentration was low.

4.4 Influence of organic aerosol

Figure 8 shows the correlation between all measurements during the campaign divided into subsets, when either no aerosol was injected or formed, mostly inorganic aerosol was present, or secondary organic aerosol (SOA) was formed

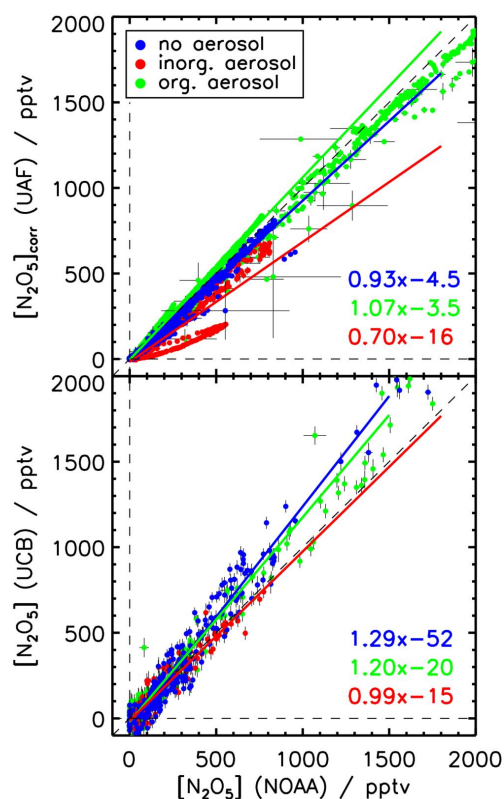


Fig. 8. Correlation between N_2O_5 data from UAF-CRDS, UCB-LIF and NOAA-CRDS depending on the presence and type of aerosol during an experiment. TMU-LIF and MPI-LIF are not shown, because instruments measured only on two days (Fig. 3). Solid lines and coloured labels give the results of the regression analysis for the different data subsets. The relationship between NOAA-CRDS and UAF-CRDS for inorganic aerosol (upper panel) falls into two parts because of the increasing deviation between measurements with increasing aerosol burden.

during VOC oxidation experiments (see Table 2). The relationship between UCB-LIF and NOAA-CRDS measurements does not depend on the presence of aerosol, consistent with the results discussed above. In this plot, UAF-CRDS data are shown without the correction, which was originally applied to account for a degradation of the inlet transmission efficiency (see above). Without this correction the data distribution becomes narrower around a line compared to the distribution with the correction shown in Fig. 3. Only the data subset that includes data when inorganic aerosol was present, still exhibits large deviations between UAF-CRDS and NOAA-CRDS, most likely because N_2O_5 is lost in the inlet system. In contrast, the difference between the data subset when no aerosol and SOA was present is small. The absolute agreement of measurements is within the range of the accuracy of instruments in these cases. Although the SOA surface concentration was within the range of values reached during experiments with inorganic aerosol (partly at similar relative humidity), exposure of SOA did not lead to a

significant N_2O_5 loss in the inlet of instruments. This is consistent with investigations of the N_2O_5 uptake coefficient in the laboratory, which show that the N_2O_5 uptake on organic aerosol can be much smaller than on inorganic aerosol (Folkers et al., 2003; Bertram and Thornton, 2009).

5 Summary and conclusions

The NO3Comp campaign brought together a large set of instruments, which are capable of detecting atmospheric NO_3 and N_2O_5 , for the first time. Eleven experiments under a variety of conditions were carried out in the simulation chamber SAPHIR in Jülich, Germany, in summer 2007. All instruments detected N_2O_5 indirectly after thermal decomposition to NO_3 , which was either detected by absorption or fluorescence, so that the sum of NO_3 and N_2O_5 mixing ratios was measured. Two CRDS instruments were equipped with separate measurement channels for simultaneous measurements of NO_3 and $\text{NO}_3 + \text{N}_2\text{O}_5$ mixing ratios. N_2O_5 mixing ratios of the other instruments were calculated by subtracting NO_3 measurements from a different instrument. However, N_2O_5 mixing ratios were typically larger than NO_3 and the differences between measurements from different instruments were small, so that the results do not depend on the choice of the NO_3 measurement.

The main results of the comparison of N_2O_5 mixing ratios are:

- There is a good agreement between measurements by all instruments within their accuracy.
- The precision of the measurements is in the low pptv range for CRDS instruments (at time resolutions between 1 s and 20 s) and 37 pptv to 63 pptv (at a time resolution of a few minutes) for the LIF instruments. These are well represented by the a priori estimated standard deviations (precision).
- The largest uncertainty in the measurements results from unaccounted changes in the N_2O_5 inlet transmission efficiency.
- The N_2O_5 inlet transmission efficiency can degrade quickly in the presence of aerosol on which N_2O_5 is taken up.
- There is no general correction that can be applied to account for a changing N_2O_5 inlet transmission efficiency over time.

The strong degradation of inlet transmission efficiencies after exposure to ammonium sulfate aerosol observed here suggests that it is necessary (1) to place a filter close to the tip of the inlet line and (2) to exchange the filter regularly on the time scale of hours. This was also shown in laboratory investigations for the NOAA-CRDS instrument (Fuchs

et al., 2008). The filter in this instrument is automatically exchanged depending on the environment, when the instrument is deployed in field measurements. Other CRDS-instruments typically use an interval for filter changes of a 1 to 4 h in field campaigns (e.g. Apodaca et al., 2008; Crowley et al., 2010). The inlet transmission efficiency needs to be characterised for an individual instrument for different conditions before it is deployed in the field.

These results show that cavity ring-down spectroscopy and laser-induced fluorescence technique can be applied for precise and accurate measurement of atmospheric N₂O₅ mixing ratios. The LIF instruments having a precision of approximately 40 pptv at a few minute time resolution, are useful for atmospheric measurement. The high precision of CRDS instruments allows detection of N₂O₅ and NO₃ in the low pptv range at a high time resolution of a few seconds.

Acknowledgements. The authors thank B. Bohn und R. Wegener for measurements of NO₃ photolysis frequencies and butanal concentrations shown in Fig. 1. The NO₃-N₂O₅-Intercomparison campaign (2007) was supported by grant no. RII3-CT-2004-505968 of the European Community within the 6th Framework Program, Section Support for research Infrastructures – Integrated Infrastructure Initiative: EUROCHAMP and Priority 1.1.6.3. Global Change and Ecosystems: ACCENT. Authors associated with University of California Berkeley would like to acknowledge support by NSF grants ATM-0639847 and ATM-0511829. Authors associated with University of Alaska Fairbanks were supported by the National Science Foundation (Grants CHE- 0094038 and ATM-0624448), as well as by the United States Department of Energy (Grant DE-FG02-03ER83695).

The service charges for this open access publication have been covered by a Research Centre of the Helmholtz Association.

Edited by: H. Herrmann

References

- Aldener, M., Brown, S. S., Stark, H., Williams, E. J., Lerner, B. M., Kuster, W. C., Goldan, P. D., Quinn, P. K., Bates, T. S., Fehsenfeld, F. C., and Ravishankara, A. R.: Reactivity and loss mechanisms of NO₃ and N₂O₅ in a polluted marine environment: Results from in situ measurements during New England Air Quality Study 2002, *J. Geophys. Res.*, 111, D23S73, doi:10.1029/2006JD007252, 2006.
- Allan, B. J., Plane, J. M. C., Coe, H., and Shillito, J.: Observations of NO₃ concentration profiles in the troposphere, *J. Geophys. Res.*, 107, 4588, doi:10.1029/2002JD002112, 2002.
- Apel, E. C., Brauers, T., Koppmann, R., Bandowe, B., Bossmeyer, J., Holzke, C., Tillmann, R., Wahner, A., Wegener, R., Brunner, A., Jocher, M., Ruuskanen, T., Spirig, C., Steigner, D., Steinbrecher, R., Gomez Alvarez, E., Müller, K., Burrows, J. P., Schade, G., Solomon, S. J., Ladstätter-Weissenmayer, A., Simmonds, P., Young, D., Hopkins, J. R., Lewis, A. C., Legreid, G., Reimann, S., Hansel, A., Wisthaler, A., Blake, R. S., Ellis, A. M., Monks, P. S., and Wyche, K. P.: Intercomparison of oxygenated volatile organic compound measurements at the SAPHIR atmosphere simulation chamber, *J. Geophys. Res.*, 113, D20307, doi:10.1029/2008JD009865, 2008.
- Apodaca, R. L.: Nocturnal processing of nitrogen oxide pollution at high latitudes: Off-axis cavity ring-down spectroscopy method development and field measurement results, Ph.d. thesis, University of Alaska Fairbanks, 2008.
- Apodaca, R. L., Huff, D. M., and Simpson, W. R.: The role of ice in N₂O₅ heterogeneous hydrolysis at high latitudes, *Atmos. Chem. Phys.*, 8, 7451–7463, doi:10.5194/acp-8-7451-2008, 2008.
- Atkinson, R. and Arey, J.: Gas-phase tropospheric chemistry of biogenic volatile organic compounds: a review, *Atmos. Environ.*, 37, S197–S219, doi:10.1016/S1352-2310(03)00391-1, 2003.
- Ayers, J. D. and Simpson, W. R.: Measurements of N₂O₅ near Fairbanks, Alaska, *J. Geophys. Res.*, 111, D14308, doi:10.1029/2006JD007070, 2006.
- Ayers, J. D., Apodaca, R. L., Simpson, W. R., and Baer, D. S.: Off-axis cavity ringdown spectroscopy: application to atmospheric nitrate radical detection, *Appl. Optics*, 44, 7239–7242, doi:10.1364/AO.44.007239, 2005.
- Ball, S. M. and Jones, R. L.: Broad-band cavity ring-down spectroscopy, *Chem. Rev.*, 103, 5239–5262, doi:10.1021/cr020523k, 2003.
- Berden, G., Peeters, R., and Meijer, G.: Cavity ring-down spectroscopy: Experimental schemes and applications, *Int. Rev. Phys. Chem.*, 19, 565–607, doi:10.1080/014423500750040627, 2000.
- Bertram, T. H. and Thornton, J. A.: Toward a general parameterization of N₂O₅ reactivity on aqueous particles: the competing effects of particle liquid water, nitrate and chloride, *Atmos. Chem. Phys.*, 9, 8351–8363, doi:10.5194/acp-9-8351-2009, 2009.
- Bohn, B., Rohrer, F., Brauers, T., and Wahner, A.: Actinometric measurements of NO₂ photolysis frequencies in the atmosphere simulation chamber SAPHIR, *Atmos. Chem. Phys.*, 5, 493–503, doi:10.5194/acp-5-493-2005, 2005.
- Brown, S. S.: Absorption spectroscopy in high-finesse cavities for atmospheric studies, *Chem. Rev.*, 103, 5219–5238, doi:10.1021/cr020645c, 2003.
- Brown, S. S., Dibb, J. E., Stark, H., Aldener, M., Vozella, M., Whitlow, S., Williams, E. J., Lerner, B. M., Jakoubek, R., Middlebrook, A. M., Gouw, J. A. D., Warneke, C., Goldan, P. D., Kuster, W. C., Angevine, W. M., Sueper, D. T., Quinn, P. K., Bates, T. S., Meagher, J. F., Fehsenfeld, F. C., and Ravishankara, A. R.: Night-time removal of NO_x in the summer marine boundary layer, *Geophys. Res. Lett.*, 31, L07108, doi:10.1029/2004GL019412, 2004.
- Brown, S. S., Neuman, J. A., Ryerson, T. B., Trainer, M., Dubé, W. P., Holloway, J. S., Warneke, C., Gouw, J. A. D., Donnelly, S. G., Atlas, E., Matthew, B., Middlebrook, A. M., Peltier, R., Weber, R. J., Stohl, A., Meagher, J. F., Fehsenfeld, F. C., and Ravishankara, A. R.: Nocturnal odd-oxygen budget and its implications for ozone loss in the lower troposphere, *Geophys. Res. Lett.*, 33, L08801, doi:10.1029/2006GL025900, 2006.
- Brown, S. S., Dubé, W. P., Osthoff, H. D., Wolfe, D. E., Angevine, W. M., and Ravishankara, A. R.: High resolution vertical distributions of NO₃ and N₂O₅ through the nocturnal boundary layer, *Atmos. Chem. Phys.*, 7, 139–149, doi:10.5194/acp-7-139-2007, 2007.

- Crowley, J. N., Schuster, G., Pouvesle, N., Parchatka, U., Fischer, H., Bonn, B., Bingemer, H., and Lelieveld, J.: Nocturnal nitrogen oxides at a rural mountain-site in south-western Germany, *Atmos. Chem. Phys.*, 10, 2795–2812, doi:10.5194/acp-10-2795-2010, 2010.
- Day, D. A., Wooldridge, P. J., Dillon, M. B., Thornton, J. A., and Cohen, R. C.: A thermal dissociation laser-induced fluorescence instrument for in situ detection of NO₂, peroxy nitrates, alkyl nitrates, and HNO₃, *J. Geophys. Res.*, 107, 4046, doi:10.1029/2001JD000779, 2002.
- Dorn, H.-P., Apodaca, R. L., Ball, S. M., Brauers, T., Brown, S. S., Cohen, R. C., Crowley, J. N., Dubé, W. P., Fry, J. L., Fuchs, H., Häsel, R., Heitmann, U., Jones, R. L., Kato, S., Kajii, Y., Kiendler-Scharr, A., Labazan, I., Langridge, J. M., Matsumoto, J., Meinen, J., Nishida, S., Platt, U., Pöhler, D., Rohrer, F., Rollins, A. W., Ruth, A. A., Schlosser, E., Schuster, G., Shillings, A. J. L., Simpson, W. R., Thieser, J., Venables, D. S., Wahner, A., Wegener, R., and Wooldridge, P. J.: Intercomparison of NO₃ radical detection instruments in the Atmosphere Simulation Chamber SAPHIR, in preparation, 2012.
- Dubé, W. P., Brown, S. S., Osthoff, H. D., Nunley, M. R., Cicora, S. J., Paris, M. W., McLaughlin, R. J., and Ravishankara, A. R.: Aircraft instrument for simultaneous, in situ measurement of NO₃ and N₂O₅ via pulsed cavity ring-down spectroscopy, *Rev. Sci. Instrum.*, 77, 034101, doi:10.1063/1.2176058, 2006.
- Folkers, M., Mentel, T. F., and Wahner, A.: Influence of an organic coating on the reactivity of aqueous aerosols probed by heterogeneous hydrolysis of N₂O₅, *Geophys. Res. Lett.*, 30, 1644, doi:10.1029/2003GL017168, 2003.
- Fry, J. L., Kiendler-Scharr, A., Rollins, A. W., Wooldridge, P. J., Brown, S. S., Fuchs, H., Dubé, W., Mensah, A., dal Maso, M., Tillmann, R., Dorn, H.-P., Brauers, T., and Cohen, R. C.: Organic nitrate and secondary organic aerosol yield from NO₃ oxidation of β-pinene evaluated using a gas-phase kinetics/aerosol partitioning model, *Atmos. Chem. Phys.*, 9, 1431–1449, doi:10.5194/acp-9-1431-2009, 2009.
- Fry, J. L., Kiendler-Scharr, A., Rollins, A. W., Brauers, T., Brown, S. S., Dorn, H.-P., Dubé, W. P., Fuchs, H., Mensah, A., Rohrer, F., Tillmann, R., Wahner, A., Wooldridge, P. J., and Cohen, R. C.: SOA from limonene: role of NO₃ in its generation and degradation, *Atmos. Chem. Phys.*, 11, 3879–3894, doi:10.5194/acp-11-3879-2011, 2011.
- Fuchs, H., Dubé, W. P., Cicora, S. J., and Brown, S. S.: Determination of inlet transmission and conversion efficiencies for in situ measurements of the nocturnal nitrogen oxides, NO₃, N₂O₅ and NO₂, via pulsed cavity ring-down spectroscopy, *Anal. Chem.*, 80, 6010–6017, doi:10.1021/ac8007253, 2008.
- Fuchs, H., Brauers, T., Häsel, R., Holland, F., Mihelcic, D., Müsgen, P., Rohrer, F., Wegener, R., and Hofzumahaus, A.: Intercomparison of peroxy radical measurements obtained at atmospheric conditions by laser-induced fluorescence and electron spin resonance spectroscopy, *Atmos. Meas. Tech.*, 2, 55–64, doi:10.5194/amt-2-55-2009, 2009.
- Fuchs, H., Ball, S. M., Bohn, B., Brauers, T., Cohen, R. C., Dorn, H.-P., Dubé, W. P., Fry, J. L., Häsel, R., Heitmann, U., Jones, R. L., Kleffmann, J., Mentel, T. F., Müsgen, P., Rohrer, F., Rollins, A. W., Ruth, A. A., Kiendler-Scharr, A., Schlosser, E., Shillings, A. J. L., Tillmann, R., Varma, R. M., Venables, D. S., Vilena Tapia, G., Wahner, A., Wegener, R., Wooldridge, P. J., and Brown, S. S.: Intercomparison of measurements of NO₂ concentrations in the atmosphere simulation chamber SAPHIR during the NO₃Comp campaign, *Atmos. Meas. Tech.*, 3, 21–37, doi:10.5194/amt-3-21-2010, 2010a.
- Fuchs, H., Brauers, T., Dorn, H.-P., Harder, H., Häsel, R., Hofzumahaus, A., Holland, F., Kanaya, Y., Kajii, Y., Kubistin, D., Lou, S., Martinez, M., Miyamoto, K., Nishida, S., Rudolf, M., Schlosser, E., Wahner, A., Yoshino, A., and Schurath, U.: Technical Note: Formal blind intercomparison of HO₂ measurements in the atmosphere simulation chamber SAPHIR during the HOxComp campaign, *Atmos. Chem. Phys.*, 10, 12233–12250, doi:10.5194/acp-10-12233-2010, 2010b.
- Geyer, A., Alicke, B., Mihelcic, D., Stutz, J., and Platt, U.: Comparison of tropospheric NO₃ radical measurements by differential absorption spectroscopy and matrix isolated electron spin resonance, *J. Geophys. Res.*, 104, 26097–26105, 1999.
- Kercher, J. P., Riedel, T. P., and Thornton, J. A.: Chlorine activation by N₂O₅: simultaneous, in situ detection of ClNO₂ and N₂O₅ by chemical ionization mass spectrometry, *Atmos. Meas. Tech.*, 2, 193–204, doi:10.5194/amt-2-193-2009, 2009.
- Kyrölä, E., Tamminen, J., Sofieva, V., Bertaux, J. L., Hauchecorne, A., Dalaudier, F., Fussen, D., Vanhellemont, F., Fanton d'Andon, O., Barrot, G., Guirlet, M., Fehr, T., and Saavedra de Miguel, L.: GOMOS O₃, NO₂, and NO₃ observations in 2002–2008, *Atmos. Chem. Phys.*, 10, 7723–7738, doi:10.5194/acp-10-7723-2010, 2010.
- Matsumoto, J., Kosugi, N., Imai, H., and Kajii, Y.: Development of a measurement system for nitrate radical and dinitrogen pentoxide using a thermal conversion/laser-induced fluorescence technique, *Rev. Sci. Instrum.*, 76, 135–141, doi:10.1063/1.1927098, 2005.
- Mihelcic, D., Klemp, D., Müsgen, P., and Pätz, H. W.: Simultaneous Measurements of Peroxy and Nitrate Radicals at Schauinsland, *J. Atmos. Chem.*, 16, 313–335, 1993.
- Orphal, J., Fellows, C. E., and Flaud, P.-M.: The visible absorption spectrum of NO₃ measured by high-resolution Fourier transform spectroscopy, *J. Geophys. Res.*, 108, 4077, doi:10.1029/2002JD002489, 2003.
- Osthoff, H., Brown, S. S., Ryerson, T. B., Fortin, T. J., Lerner, B. M., Williams, E. J., Pettersson, A., Baynard, T., Dubé, W. P., Cicora, S. J., and Ravishankara, A. R.: Measurement of atmospheric NO₂ by pulsed cavity ring-down spectroscopy, *J. Geophys. Res.*, 111, D12305, doi:10.1029/2005JD006942, 2006.
- Osthoff, H., Roberts, J. M., Ravishankara, A. R., Williams, E. J., Lerner, B. M., Sommariva, R., Bates, T. S., Coffman, D., Quinn, P. K., Dibb, J. E., Stark, H., Burkholder, J. B., Talukdar, R. K., Meagher, J., Fehsenfeld, F. C., and Brown, S. S.: High levels of nitryl chloride in the polluted subtropical marine boundary layer, *Nat. Geosci.*, 1, 324–328, doi:10.1038/ngeo177, 2008.
- Paul, J. B., Lapson, L., and Anderson, J. G.: Ultrasensitive absorption spectroscopy with a high-finesse optical cavity and off-axis alignment, *Appl. Optics*, 40, 4904–4910, doi:10.1364/AO.40.004904, 2001.
- Phillips, G. J., Tang, M. J., Thieser, J., Brickwedde, B., Schuster, G., Bohn, B., Lelieveld, J., and Crowley, J. N.: Significant concentrations of nitryl chloride observed in rural continental Europe associated with the influence of sea salt chloride and anthropogenic emissions, *Geophys. Res. Lett.*, 39, L10811, doi:10.1029/2012gl051912, 2012.

- Platt, U., Perner, D., Winer, A. M., Harris, G. W., and Pitts, J. N.: Detection of NO₃ in the polluted troposphere by differential optical absorption, *Geophys. Res. Lett.*, 7, 89–92, doi:10.1029/GL007i001p00089, 1980.
- Press, W. H., Teukolsky, S. A., Vetterling, W. T., and Flannery, B. P.: Numerical recipes in C, Cambridge University Press, 2nd Edn., 1992.
- Ridley, B. A., Grahek, F. E., and Walega, J. G.: A small, high-sensitivity, medium-response ozone detector suitable for measurements from light aircraft, *J. Atmos. Ocean. Tech.*, 9, 142–148, doi:10.1175/1520-0426(1992)009;0142:ASHSMR;2.0.CO;2, 1992.
- Riemer, N., Vogel, H., Vogel, B., Schell, B., Ackermann, I., Kessler, C., and Hass, H.: Impact of the heterogeneous hydrolysis of N₂O₅ on chemistry and nitrate aerosol formation in the lower troposphere under photochemical conditions, *J. Geophys. Res.*, 108, 4144, doi:10.1029/2002jd002436, 2003.
- Rohrer, F., Bohn, B., Brauers, T., Brüning, D., Johnen, F.-J., Wahner, A., and Kleffmann, J.: Characterisation of the photolytic HONO-source in the atmosphere simulation chamber SAPHIR, *Atmos. Chem. Phys.*, 5, 2189–2201, doi:10.5194/acp-5-2189-2005, 2005.
- Rollins, A. W., Kiendler-Scharr, A., Fry, J. L., Brauers, T., Brown, S. S., Dorn, H.-P., Dubé, W. P., Fuchs, H., Mensah, A., Mentel, T. F., Rohrer, F., Tillmann, R., Wegener, R., Wooldridge, P. J., and Cohen, R. C.: Isoprene oxidation by nitrate radical: alkyl nitrate and secondary organic aerosol yields, *Atmos. Chem. Phys.*, 9, 6685–6703, doi:10.5194/acp-9-6685-2009, 2009.
- Schlosser, E., Bohn, B., Brauers, T., Dorn, H.-P., Fuchs, H., Häsel, R., Hofzumahaus, A., Holland, F., Rohrer, F., Rupp, L. O., Siese, M., Tillmann, R., and Wahner, A.: Intercomparison of two hydroxyl radical measurement techniques at the atmosphere simulation chamber SAPHIR, *J. Atmos. Chem.*, 56, 187–205, doi:10.1007/s10874-006-9049-3, 2007.
- Schlosser, E., Brauers, T., Dorn, H.-P., Fuchs, H., Häsel, R., Hofzumahaus, A., Holland, F., Wahner, A., Kanaya, Y., Kajii, Y., Miyamoto, K., Nishida, S., Watanabe, K., Yoshino, A., Kubistin, D., Martinez, M., Rudolf, M., Harder, H., Berresheim, H., Elste, T., Plass-Dülmer, C., Stange, G., and Schurath, U.: Technical Note: Formal blind intercomparison of OH measurements: results from the international campaign HOxComp, *Atmos. Chem. Phys.*, 9, 7923–7948, doi:10.5194/acp-9-7923-2009, 2009.
- Schuster, G., Labazan, I., and Crowley, J. N.: A cavity ring down/cavity enhanced absorption device for measurement of ambient NO₃ and N₂O₅, *Atmos. Meas. Tech.*, 2, 1–13, doi:10.5194/amt-2-1-2009, 2009.
- Simpson, R. J.: Continuous wave cavity ring-down spectroscopy applied to in situ detection of dinitrogen pentoxide (N₂O₅), *Rev. Sci. Instrum.*, 74, 3442–3452, doi:10.1063/1.1578705, 2003.
- Slusher, D. L., Huey, L. G., Tanner, D. J., Flocke, F. M., and Roberts, J. M.: A thermal dissociation-chemical ionization mass spectrometer (TD-CIMS) technique for the simultaneous measurement of peroxyacyl nitrates and dinitrogen pentoxide, *J. Geophys. Res.*, 109, D19315, doi:10.1029/2004JD004670, 2004.
- Thornton, J. A., Kercher, J. P., Riedel, T. P., Wagner, N. L., Cozic, J., Holloway, J. S., Dubé, W. P., Wolfe, G. M., Quinn, P. K., Middlebrook, A. M., Alexander, B., and Brown, S. S.: A large atomic chlorine source inferred from mid-continental reactive nitrogen chemistry, *Nature*, 464, 271–274, doi:10.1038/nature08905, 2010.
- Wagner, N. L., Dubé, W. P., Washenfelder, R. A., Young, C. J., Pollack, I. B., Ryerson, T. B., and Brown, S. S.: Diode laser-based cavity ring-down instrument for NO₃, N₂O₅, NO, NO₂ and O₃ from aircraft, *Atmos. Meas. Tech.*, 4, 1227–1240, doi:10.5194/amt-4-1227-2011, 2011.
- Wayne, R. P., Barnes, I., Biggs, P., Burrows, J. P., Canosa-Mas, C. E., Hjorth, J., Bras, G. L., Moortgat, G. K., Perner, D., Poulet, G., Restelli, G., and Sidebottom, H.: The nitrate radical – physics, chemistry and the atmosphere, *Atmos. Environ.*, 25, 1–203, 1991.
- Wood, E. C., Wooldridge, P. J., Freese, J. H., Albrecht, T., and Cohen, R. C.: Prototype for in situ detection of atmospheric NO₃ and N₂O₅ via laser-induced fluorescence, *Environ. Sci. Technol.*, 37, 5732–5738, doi:10.1021/es034507w, 2003.
- Wood, E. C., Bertram, T. H., Wooldridge, P. J., and Cohen, R. C.: Measurements of N₂O₅, NO₂, and O₃ east of the San Francisco Bay, *Atmos. Chem. Phys.*, 5, 483–491, doi:10.5194/acp-5-483-2005, 2005.
- Wooldridge, P. J., Perring, A. E., Bertram, T. H., Flocke, F. M., Roberts, J. M., Singh, H. B., Huey, L. G., Thornton, J. A., Wolfe, G. M., Murphy, J. G., Fry, J. L., Rollins, A. W., LaFranchi, B. W., and Cohen, R. C.: Total Peroxy Nitrates (ΣPNs) in the atmosphere: the Thermal Dissociation-Laser Induced Fluorescence (TD-LIF) technique and comparisons to speciated PAN measurements, *Atmos. Meas. Tech.*, 3, 593–607, doi:10.5194/amt-3-593-2010, 2010.
- Yokelson, R. J., Burkholder, J. B., Fox, R. W., Talukdar, R. K., and Ravishankara, A. R.: Temperature dependence of NO₃ absorption spectrum, *J. Phys. Chem.*, 98, 13144–13150, 1994.